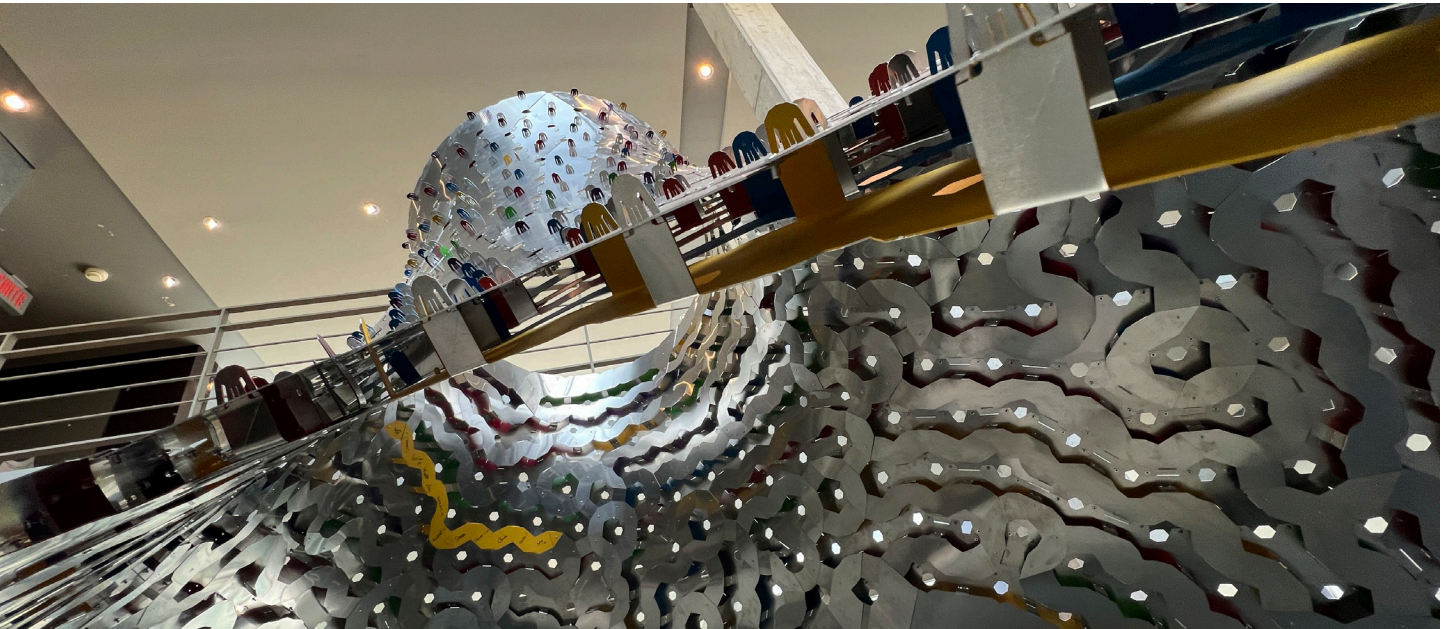**LEAVE THIS PAGE BLANK
DO NOT DELETE THIS PAGE**

The Cnidaria Pavilion

A new structural and assembly system
for load bearing, architectural "deep-skins"

Andrei Nejur
University of Montreal, LAIR

Szende Szentesi
Laval University

Reza Taghavifard
University of Montreal, LAIR

Thomas Balaban
University of Montreal

Patrick Harrop
University of Montreal

1

ABSTRACT

Cnidaria is a research pavilion developed in the University of Montreal, School of
Architecture ARC 6801H research master's studio and unveiled in May 2024. This 25 sqm
shell showcases an innovative method for constructing large-span, doubly curved, load-
bearing architectural surfaces using low-tech manual folding and snap-fit assembly. Its
design, inspired by sea anemones, and sound focusing acoustic shells, emerged from a
soap-bubble membrane simulation that optimizes material use by evenly distributing struc-
tural stress across the surface.

Constructed from dual layers of 1mm-thick aluminum stripes, Cnidaria's outer layer acts
as a structural and aesthetic membrane, providing its shelter function and handling axial
loads. The inner layer, sparsely arranged, addresses bending and shearing stresses, with
a biologically inspired pattern that educates and enhances the aesthetic. This approach
combines lightweight, aesthetic qualities with structural integrity through a novel snap-fit
connection that allows for easy assembly without requiring inter-layer access.

The workflow employs novel, cutting-edge algorithms to efficiently segment complex
curved geometries into non-overlapping, clash-free stripes, streamlining the design
process. The constructed shell serves as a projection screen for digital art, highlighting its
dual function as an electronic arts venue.

1   Detail view of the Cnidaria
    Pavilion showing the double
    layer system and the snap-fit
    connections.

INTRODUCTION

The design and construction of complex architectural surfaces are challenging tasks that require a balance between artistic vision, material properties, and engineering constraints. The use of discretization, or the segmentation of large surfaces into smaller components, is often indispensable in bringing ambitious architectural designs to life. Discretization allows architects to work within the constraints imposed by materials, fabrication processes, transport logistics, and assembly requirements (Eigensatz et al. 2010). However, discretization also introduces challenges, necessitating innovative solutions to ensure the final structure is aesthetically pleasing, structurally sound, economically viable and most of all possible to assemble.

The Necessity of Discretization

Discretization is a critical tool for managing costs and construction timelines, as well as achieving specific design objectives. By breaking down a complex curved surface into manageable parts, architects can leverage planar sheet materials to approximate challenging geometries. This approach maximizes the efficiency of fabrication and assembly by enabling the use of standardized, affordable materials while minimizing waste. The result is a form that can be constructed easier and more affordable.
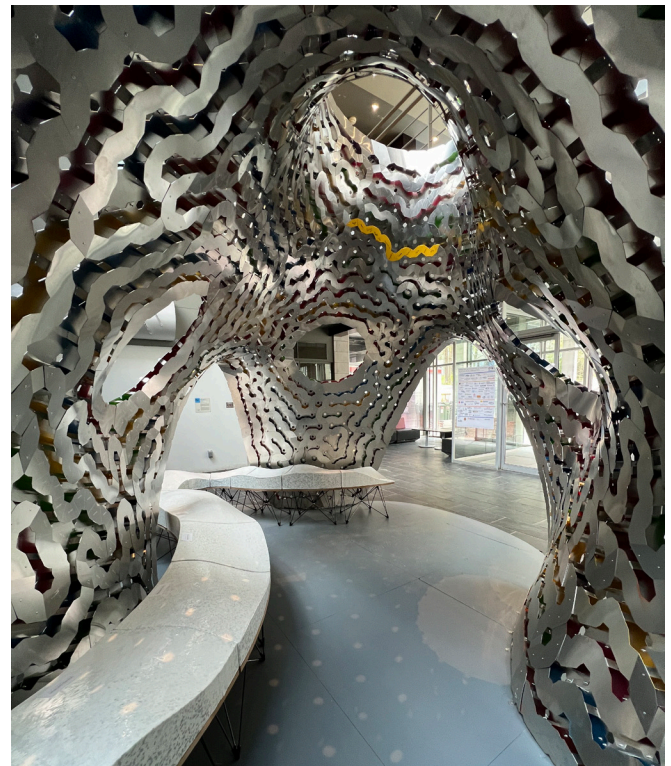
However, discretization is not a one-size-fits-all solution. It requires striking a balance between achieving a feasible form and maintaining aesthetic integrity. Oversegmentation can lead to an unmanageable multiplication of parts and unreasonably long assembly times. Conversely, too few segments may compromise the structure's curvature or stability. Additionally, different methods of discretization have unique implications. For instance, planar quadrilateral (PQ) meshes (Pottmann 2013) and ruled surface rationalizations (Flöry and Pottmann 2010) offer fabrication-friendly approaches due to their planarity and unfolding capabilities but limit the range of possible forms.

Shortcomings and Challenges of Discretization

Despite its necessity and advantages, discretization introduces a range of structural, aesthetic, and logistical challenges. One of the primary structural concerns is material discontinuity. This discontinuity introduces fault lines where the individual segments are joined, compromising the material coherence of the overall structure. This can lead to structural vulnerabilities that are difficult to mitigate. While multilayered surfaces(Fornes 2016; Stanojevic and Takahashi 2019), discrete piece overlaps (Schleicher et al. 2015; La Magna, Schleicher, and Knippers

2

3

2 General view of the pavilion showing the difference between the outer and inner layers.

3 Interior view of the pavilion showing the oculus and the openings in the shell.

2016), finger joints (Magna et al. 2013), structural assembly connectors [Blinded reference] and other specialized connection techniques can help alleviate these issues, they cannot fully replicate the structural continuity of a monolithic surface and introduce specific additional issues like increased assembly difficulty and time.

Architects must also contend with geometric deviations that arise from the approximation of curved surfaces. The segmented components of a discretized structure can deviate significantly from the original design intent, especially when subjected to structural loads. While these deviations can often be simulated digitally and accounted for in the design process, this isn't always straightforward. Minimizing deviations typically involves increasing the number of smaller segments or deforming individual parts through bending or rolling (Rossi and Nicholas 2018). This approach, however, can raise costs due to increased assembly complexity or the need for additional guidance mechanisms during fabrication.

Moreover, uncontrolled deformations resulting from material discontinuity can have significant aesthetic and structural impacts, potentially leading to defects that undermine the project's visual appeal and functional performance. Addressing these challenges often requires expensive and computationally intensive simulations during design, and meticulous craftsmanship during construction.

Other drawbacks include the added weight of connection components and aesthetic limitations caused by the necessary seams between segments. These seams can disrupt the architectural image or necessitate further design measures to obscure them.

Supported and Self-Supported Surfaces

The advantages and challenges of discretization are relevant to both self-supporting surfaces (which carry their own loads) and supported surfaces (which rely on an external structural network). Self-supporting surfaces often rely on inherent material properties and additional structural features such as folds, active bending (Lienhard and Knippers 2015), curvature (Martín-Pastor and García-Alvarado 2019), and multiple layers (Nicholas et al. 2016) to achieve the necessary rigidity. Notable exceptions include inflatable structures that utilize internal pressure to maintain their form (Ayres, Vestartas, and Ramsgaard Thomsen 2018).

These strategies for reinforcing the structure through surface features help create rigidity without compromising the surface's aesthetic. However, they are constrained by the properties of the chosen materials, and the resulting aesthetics are often tied to specific structural forms. If the design requires different proportions or higher structural demands, additional reinforcement becomes necessary.

Supported surfaces, by contrast, rely on external structural networks that resolve the collection and transfer of loads to the supporting elements (Schling 2018). This additional support structure complicates the design, fabrication, and assembly processes, particularly when working with thin sheet materials that are prone to deformation. The surface-to-structure connection strategy is also crucial and can add weight, complexity, and cost (Schmieder and Mehrtens 2013).

Hybrid solutions and multi-layer shells

In (Nejur 2023) a hybrid solution is proposed that combines structural reinforcement with the assembly tabs and assembly guides to significantly improve stiffness of self-supported structural skins. Even if the system has many advantages, producing a large curved self-supported skin using only thin-sheet aluminum it still had several important shortcomings like lateral load vulnerability, increased assembly time and limited assembly reach while working inside the open cells. This limited reach is one of the reasons why flat sheet multi-layer shells, regardless of material, have been used sparingly in the construction industry in the last decades. With some exceptions, like pre-made thin sheet "bricks" (Bechert et al. 2021) that can be assembled from the outside before being integrated in the shell, working with multiple spaced-out layers is cumbersome due to the limited reach inside the structure. Despite these challenges, the volumetric nature of dual layer shells with space between the layers makes them an ideal solution to tackle simultaneously the divergent constraints of stiffness and weight usually associated with structural skin constructions from thin sheet materials.

PROBLEM STATEMENT

The construction of architectural structures from thin sheet materials is fraught with significant challenges. Chief among these is the delicate balance between stiffness and weight, particularly in self-supporting surfaces where, enhancing structural rigidity often results in increased material weight, complicating assembly, and elevating costs. Additionally, structures that rely on supplementary frameworks to achieve necessary support encounter complexities that can detract from aesthetic intentions and inflate both budget and construction timelines. Moreover, dual-layer structures, despite their potential for aesthetic and functional enhancement, present formidable assembly challenges due to limited access between layers, thereby

increasing the likelihood of assembly errors and extending project durations. These prevalent issues underscore a critical gap in the current methodologies employed for constructing large-scale, self-supporting architectural surfaces from thin materials. This gap necessitates a novel approach that harmonizes structural integrity, aesthetic flexibility, and assembly efficiency, thereby advancing the architectural possibilities of thin sheet materials.

PROPOSED RESEARCH

In this paper we propose a novel construction method for large scale doubly curved self-supported architectural surfaces. The proposed process extends the hybrid method of integrating the discreet part assembly with the structural optimization proposed in (Nejur 2023) to dual layer "deep skins". We propose a multi-step process that can work with a large variety of doubly curved surfaces. First a triangular mesh representation of the input is offset producing two topologically identical layers, a base layer, and a support layer. Using newly proposed algorithms, the layers are independently decomposed, subdivided, and transformed according to structural and fabrication criteria, while the topological relationship between the layers is conserved. The base layer is assembled in sectors and the support layer is added using a new snap-fit interlayer connection. Finally, the sectors are assembled and stiffened with a series of bridge connections.
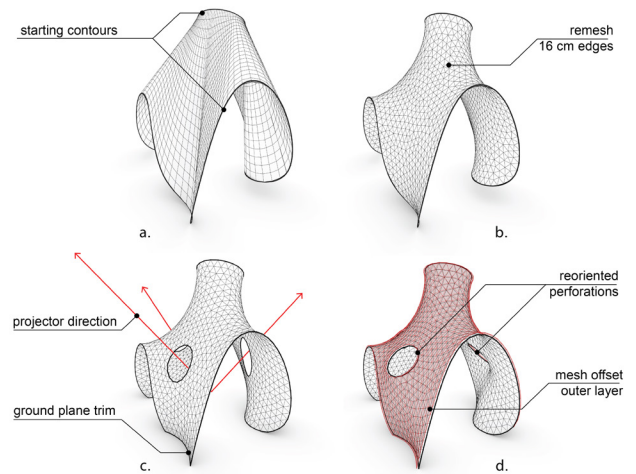
METHODOLOGY

General form-finding

The general shape of the shell is created through an iterative form finding process based on the Kangaroo extension of Grasshopper using a soap bubble simulation goal tasked with finding the minimal area between two given splines. The pavilion was placed inside the building of the Faculty of Environmental Design in a relatively well traveled space. As a result, the input splines defining the general limits of the shape were modelled by the students to trace 3 accesses inside the shell as well a funnel type oculus tasked with bringing in sound from a nearby walkway. To produce the shell, a simple loft between the base spline and the oculus spline was meshed and then relaxed with kangaroo using the live soap bubble goal as shown in Figures 4.a and 4.b. The relaxed mesh was tweaked to have a flat base before three more perforations were added to match the directions of three video projectors that would be hung in the space of the faculty entry hall facing the shell. Figure 4.c shows the result of the process.

The base layer

The perforated mesh was relaxed again as a soap bubble membrane this time between the five naked boundaries
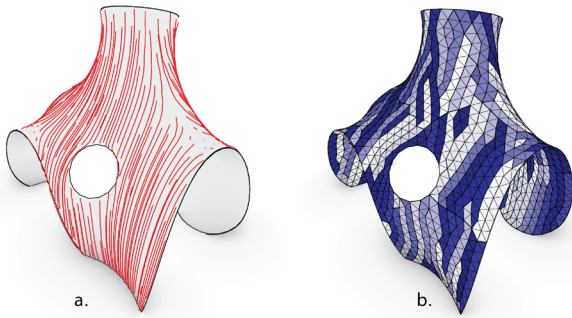

4   Form-finding of the shell.

of the perforated mesh (the twisting base, the oculus ring and the three new perforations). To add additional double curvature to the shell the naked boundaries corresponding to the three perforations were offset slightly during the relaxation process along the projector axes and rotated to be perpendicular to those axes. This ensured that curvature related stiffness was a lot more prevalent in the shell than in the original un-perforated version. The result is re-meshed at several steps using the Grasshopper in-built TriRemesh tool to have quasi-equal triangular faces with edge lengths around 16 cm. This value was found to be optimal for hand assembly. Figure 4.b shows the remeshing result after the initial form relaxation with kangaroo.
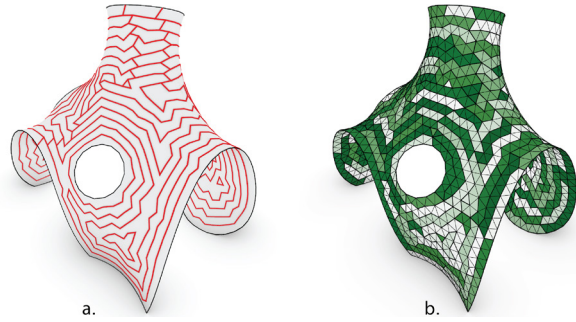
To create the "deep skin" the base shell mesh is offset 40 mm outwards using a custom algorithm capable of individually moving mesh vertices in the direction of their respective normals by a custom amount. The offset algorithm is also tasked with keeping the vertices initially on the ground plane (i.e. have the Z coordinate = 0) on the same ground plane. This ensures that no mesh split, or Boolean operations are necessary to keep the feet of the shell flat and on the ground while the two shell layers remain topologically equivalent. This last aspect is consequential for the decomposition, fabrication and for the subsequent assembly of the two-layer shell. It is also important for the rigidity of the individual layers, and most importantly for the creation of the interlayer connections. Figure 4.d shows the final shape of the shell and the relative distance between the layers.

The outer layer

Architecturally, the outer layer is supposed to fulfill a protection/projection function. First it checks the basic

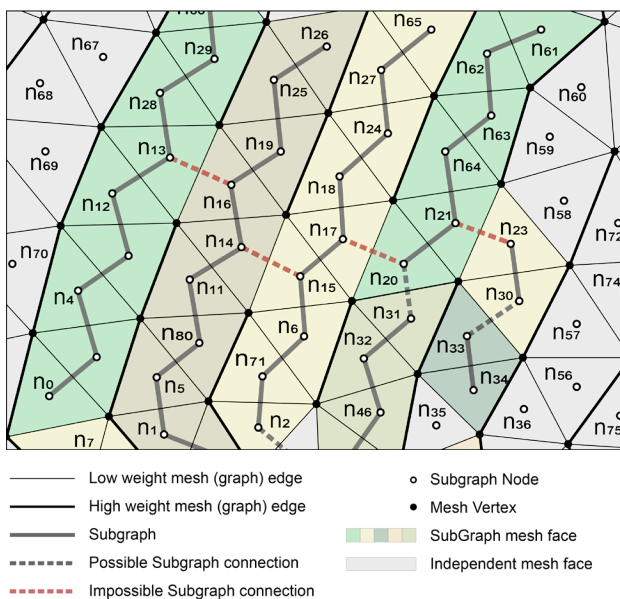a.   b.

a.   b.

shelter demand of most architectural spaces, that is to create a certain separation (in this case mostly visual) between the interior and the exterior. Second, the outer membrane fulfills the projection screen function for the three video projectors. To fulfill this task the outer layer decomposition worked with an opaque, minimally perforated skin without visible connection flaps.

Structurally, the continuous nature of the membrane, coupled with the quasi-funicular shape of the pavilion made the outer layer a good candidate to tackle axial forces in the shell. To support this approach, we decided to decompose the mesh in a series of strips aligned with the highest descent directions on the mesh traced using the mesh-flow algorithm. The mesh decomposition uses the Ivy Grasshopper extension and works on the dual graph of the mesh based on precomputed weight as explained in (Nejur and Steinfeld 2016; 2017). The graph edge weight is computed based on the angle deviation of the graph edge direction from the tangent calculated at the closest point on a set of curves resting on the mesh a using a similar algorithm as in (Nejur 2023). Differently from that paper the curves in this case are computed using a water flow
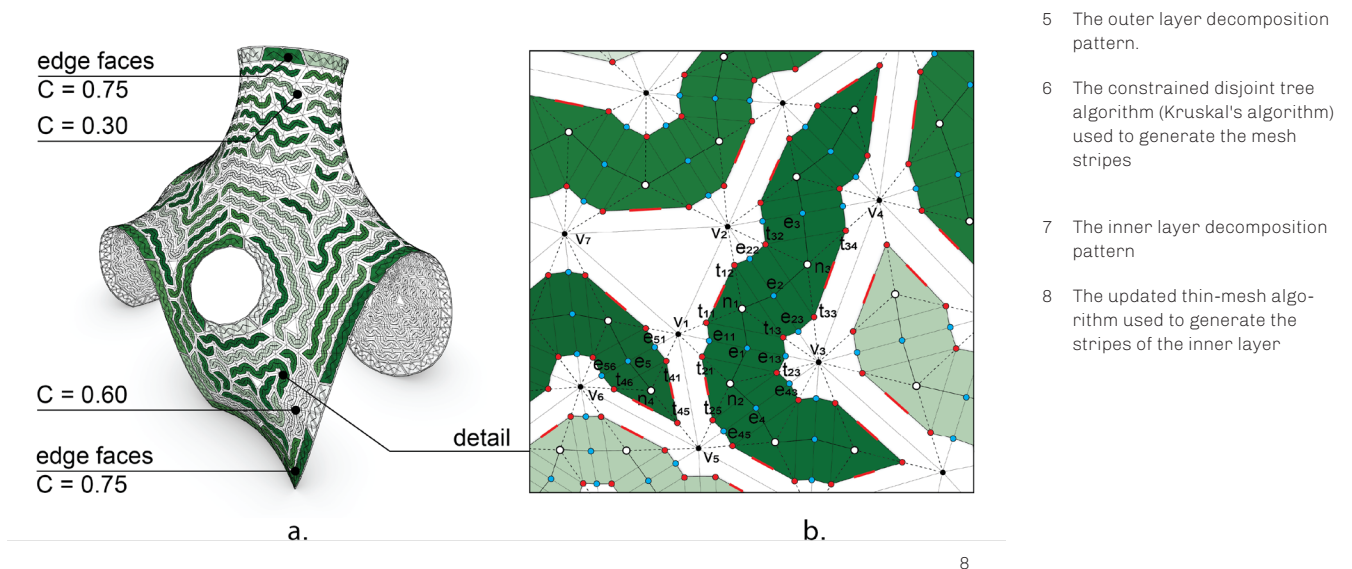
algorithm similar to (Rueda, Noguera, and Martínez-Cruz 2013). The resulting weight landscape gives any decomposition solution a bias towards creating tree graphs that climb or descend the mesh following the steepest gradient available. Figure 5.a shows the curves produced by the water-flow algorithm and Figure 5.b the resulting mesh decomposition.

As an evolution from the mesh-walker solution employed in (Nejur 2023) the present decomposition algorithm uses a new constrained, disjoint-set algorithm (Kruskal's algorithm) that works on the same base as the original Ivy algorithm but adds a series of optional limitations when fusing the disjoint elements of the set to create larger subgraphs. First, a sparse option limits the joining of sub-graphs if they share more than two mesh topological vertices (the topological vertices of the mesh edge dual to the graph edge that was selected for processing). Second, a max valence setting (2 in our case) limits any sub-graph joining if the graph nodes defining the processed edge would end up with a larger valence than the maximum allowed value after joining

The new algorithm works instantly on the mesh and produces quantitatively similar strips compared with the mesh-walker algorithm. Figure 6 depicts the typical constraints of the algorithm during the process of tree graph construction. Subgraphs $S(n1, n5, n80, n11, n14, n16, n19, n25, n26)$, $S(n2, n71, n6, n15, n14, n17, n18, n24, n24, n27, n65)$ could be joined into a larger subgraph through the edge $E(n14, n15)$. The edge could be a valid candidate for the normal Kruskal algorithm as it has a low weight as shown by the thin mesh edge representing it. The potential graph edge is represented however with a dotted orange line as it is not a valid connection as per the sparsity and valence constraints. The two subgraphs already share more than the maximum of two mesh vertices (the black dots) and if connected, nodes $n14$ and $n15$, would have a valence of 3, thus larger than the maximum prescribed of 2 graph edges per node. In another example $S(n30, n23)$ can use edge $E(n33, n30)$ or $E(n23, n21)$ to either be joined

—— Low weight mesh (graph) edge	○ Subgraph Node
—— High weight mesh (graph) edge	● Mesh Vertex
—— Subgraph	SubGraph mesh face
···· Possible Subgraph connection	Independent mesh face
···· Impossible Subgraph connection	

edge faces
C = 0.75

C = 0.30

C = 0.60

edge faces
C = 0.75

detail

a.

b.

8

to *S(n33,n34)* or *S(n20, n64, n63, n62, n61)*. As shown in the figure only the first connection is valid as the second connection would give *n21* a valence of 3.

The inner layer.

The inner layer is dependent on the outer layer but has an equally important structural scope. It is designed to reinforce the shell against shearing force and bending moment by adding a virtual depth to the 1mm membrane. The geometry of the inner shell is created in several steps: decomposition, mesh-thinning, and connector generation.

The decomposition step functions in a similar way to the decomposition of the outer layer, but it uses a different weight landscape for the mesh graph. In this case the weight is computed using the orange peel algorithm of Ivy as described in (Nejur and Steinfeld 2017). For this use the peel effect is generated starting from the vertices of the naked edges associated with the three perforations oriented towards the video projectors as shown in Figure 7.a. On the generated weight landscape, the same modified Kruskal algorithm used on the outer layer produces a series of strips in concentric patterns rippling away from the perforations as shown in Figure 7.b.
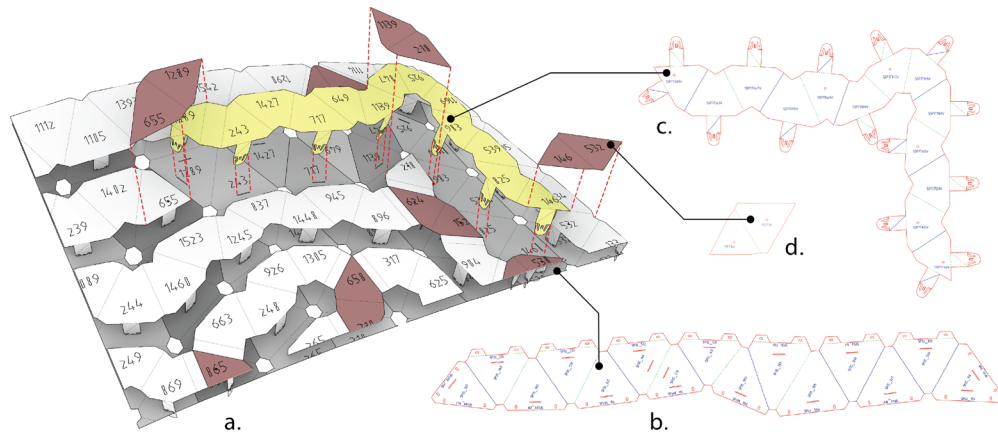
The mesh thinning step of the inner layer was required for several reasons: assembly access (full layers on both sides of the inter-layer space would impede assembly), connector fabrication (to reduce assembly time and increase stiffness the connectors had to be prefabricated as part of the inner layer through the laser-cutting process), and weight reduction (reducing the coverage of the underside layer reduces the weight without a significant sacrifice in stiffness)

To achieve this step, we used the "thin mesh" tool of Ivy

for Grasshopper that offsets each vertex of the mesh face towards the face center based on a thinning coefficient and creates additional mesh quads for the mesh edges to connect the now isolated mesh faces. Because it uses the Ivy system the mesh thinning algorithm replicates the connectivity of the mesh subgraph in the new "thinned" result.

The updated version of the algorithm we used for the presented research was able to use custom thinning coefficients (*C* values) assigned to mesh graph nodes thus allowing us to modulate the material use and stiffness throughout the structure. All faces touching naked vertices were assigned a *C* value of 0.75 while all other faces were assigned a value between 0.6 and 0.3 depending on the height (the Z coordinate) of the mesh face centroid. Figure 8.a shows the impact the C value has on the width of the thinned mesh strips. In Figure 8.b one can see how the thinned strips are constructed. For each graph node the vertices of the base mesh triangle are connected to the triangle centroid. For example, *n1* is connected to *v1*, *v2* and *v3*. Using the *C* value for the graph node (*Cn1*), points *t11*, *t12* and *t13* are determined inside the face. These are the vertices of the new thinned mesh face *T(t11, t12, t13)*. Using the location of the edge center for the two edges connected to node *n1* (*e1* and *e2*), and the *C* values for the same edges $Ce1 = (Cn1 + Cn3)/2$ and $Ce2 = (Cn1 + Cn2)/2$, the points *e22*, *e23*, *e11* and *e13* are determined on the lines connecting *e2* with *v2* and *v3* and *e1* with *v1* and *v3*. These points are used to construct two quad mesh faces *Q(t12, t13, e22, e23)* and *Q(t11, t13, e11, e13)* that will link the thinned triangle face with other faces.

Connector generation. As a result of these operations, the naked edges in the original strips remain naked edges in

a.

b.

c.

d.

9

the "thinned" version and move towards the center of the original mesh face. By placing the inter layer connectors as extra mesh geometry connected to the naked edges (the red lines in Figure 8.b.), we were able to create links between the outer and inner layers that could be fabricated in the same cutting process as the strips in the inner layer. See Figure 9.c for the full geometry of the thinned mesh with the connectors. During the assembly process the connectors can be engaged simply through manual bending towards the outer layer. The inner offset, part of the "mesh thinning" process, ensures that any meeting point between the connectors and the outer layer does not clash with possible connections between the strips of the outer layer.

The connectors are composed of two extra triangular faces that connect to the naked edge and are oriented towards the outer layer. To simplify the assembly process, the connector geometry uses a single 3 cm width. This is resolved by subdividing the naked edge to obtain a 3 cm sub-curve in its middle. At the end of the added geometry a snap-fit connection is attached. The snap-fit connection is designed to be inserted into a rectangular perforation located on the corresponding outer layer mesh face. The perforation is positioned similarly to the red line in Figure 8.b but in the corresponding face in the outer layer. The perforations can be observed in the strip shown Figure 9.b.

The 2.1-layer system.
The inner layer strips connect to the outer layer using the connectors spawning from the naked edges of the thinned mesh. Each naked edge in the original mesh decomposition of the inner layer spawns one connector. More naked edges equal more connections between the layers. The proposed inner layer segmentation manages to maximize the number of connections ensuring that each face of the original inner layer has at least one connection to its outer layer equivalent. Leaf faces (the ones that have only one edge connection inside the strip) have two naked edges

and thus two connectors to the outer layer. The downside of this naked edge connection strategy is that many naked edges for each strip produces more disconnection between the faces of the inner layer. This induces potential bending issues perpendicular to the direction of the inner strips. To compensate for this weakness a series of in-layer connections (bridges) was proposed. The bridges are short strips of thinned mesh constructed to span between the strips of the inner layer, based on the graph edges initially cut by the segmentation algorithm. From the cut graph edges a subset is selected so that each edge connects one leaf node from one strip to a neighboring strip. Another subset of edges is selected so that graph nodes with a depth (i.e., the topological distance to a leaf node) larger than 7 are connected to neighboring strips. This extra partial layer covers all potentially dangerous sharp leaf nodes while increasing bending stiffness for the direction perpendicular to the strips. In total, over 250 bridges were produced by the algorithm. Figure 9.a shows how the bridges attach to the inner layer once the latter is fitted to the outer layer. In total the bridges cover less than 10% of the number of faces in the original mesh hence the 2.1 layer system.

The 2.1-layer system was designed to be simple to fabricate and fast to assemble. To facilitate manual assembly, sizes were limited. First, strips were limited to a maximum length of 15 base-mesh faces. Second, the 25 sqm surface of the shell was divided into 12 similarly sized segments that could be comfortably handled by a two-person assembly team. The assembly sequence of a segment involved 3 simple steps: 1. Assembly of the outer layer strips using rivets (Figure 10.a), 2. Folding the connectors and fitting the inner layer strips onto the outer layer (Figure 10.b,c), 3 Adding the segment bridges between inner layer strips using rivets (Figure 10.d). Once all the segments were constructed, they were put together following a similar logic.
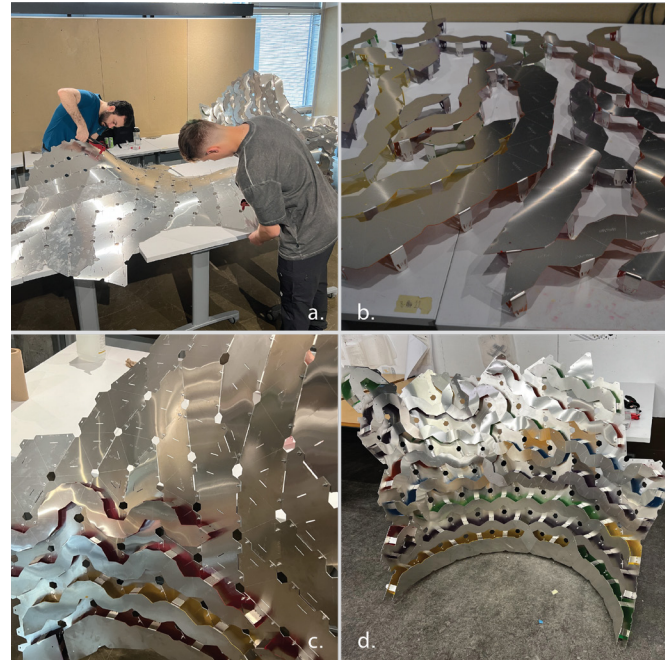
FEA analysis.

Before assembly, to validate the structural advantages of the dual layer shell, a simplified FEA analysis was performed on the pavilion using the Grasshopper add-on Karamba. For comparison similar tests were first performed on a single layer structure and then on the dual layer structure. To facilitate the analysis of the dual layer structure, the connection between the two layers was simplified using 3-valence mesh edges that replaced the snap-fit connection system. Two testing scenarios were used for each structure. The first scenario involved a uniformly distributed dead load equivalent to 2 times the weight of the shell. The second scenario included, additionally to the dead load, two 1kN live loads pushing horizontally on the side of the pavilion. All other test parameters were identical, and the two shells were considered as continuous 1mm aluminum 5025H32 alloy.

The single layer shell performed decently under the 126 kg dead load. It displayed a maximum deflection of 12 cm as shown in Figure 11.a. Under the combined dead and live loads, however, the structure was heavily deformed with a maximum deflection of over 115 cm. The deformation was likely beyond the collapse point, as the Karamba evaluation algorithm we used was not developed to handle large deformations. Figure 11.b shows the deformation of the shell in this loading scenario. The actual deformation is reduced to 50% to keep the original form discernible.

The double layer shell fared much better in both tests. Under the 220 kg dead load the deflection was invisible (only 0.3 cm). Under the combined dead and live load, the structure showed only a 2 cm local deformation where the live loads were applied with no deformation for the overall structure. Figure 11.c shows the combined loading scenario for the double shell with the deformation almost invisible in the image.

DISCUSSION AND NEXT STEPS

The digital workflow was supported by series of in-depth material investigations that targeted several important directions. Connection development, assembly process validation and empirical structural testing. The first two directions could be investigated fully in partial or smaller scale prototype and as such they yielded important information that produced the snap-fit connection, the flat flap connection between the strips of the outer layer, and a very rapid assembly sequence for the sectors. Only 2 hours were required per sector for a two-person team including riveting. Empirical structural testing carried out on the same partial prototypes produced a good understanding of the 2.1-layer system albeit an incomplete one. The summed
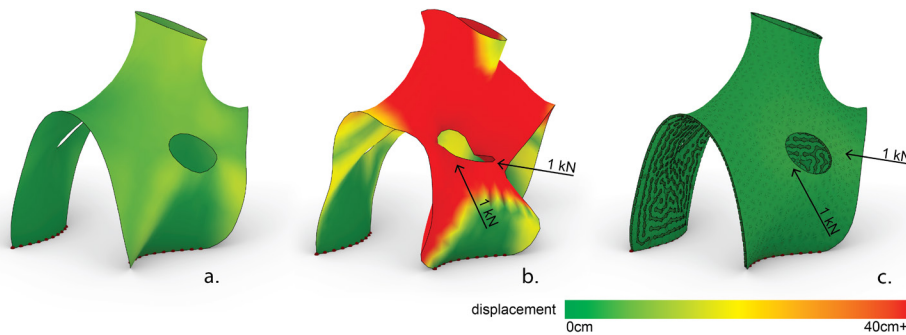
limited rotational freedom of the several thousands snap-fit connections in the system, that was impossible to simulate in the FEA analysis, resulted in a more flexible than expected shell. In future studies stiffer connections (including riveted ones) will be investigated together with larger and more variable distances between the layers. A new, more accurate FEA model will also be employed to predict structural behaviors.

The selection of the cut edges in the inner layer merits further investigation too. In the present research the decomposition of the inner layer was programmatic and based mostly on an aesthetic bias. The only structural concern was having the strips of the inner layer oriented differently between layers. Additionally, opting for strips in the inner layer gave ample inter-layer connection possibilities (i.e., through the multiple naked edges of the strips) but introduced a disconnection in the inner layer that left the shell more flexible if bent perpendicular to the chosen strip direction. This was addressed partially by the inclusion of the bridges as an additional partial layer. In a forthcoming publication we plan to address this more thoroughly with a genetic algorithm that can efficiently investigate the solution space of mesh edge disconnection and its direct effect on the structural behavior of the shell.

CONCLUSION

In this paper we have shown a novel technique for the construction of load bearing, large-span, architectural scale, doubly curved surfaces built exclusively from ultra-thin sheet metal. The construction technique is based on a 2.1-layer system with a snap-fit inter-layer connection that

11 Structural simulation showing the displacement of a single layer shell (a,b) compared with the proposed double layer system (c)

12 Outside view of the pavilion.

13 Outside view of the pavilion showing the seating

makes the assembly extremely fast without the requirement of a skilled workforce or costly power tools. The resulting shell shown in Figure 10 is lightweight (only 220 kg for 25 sqm) and stiff enough to support additional weight, making it an interesting alternative for the existing formwork solutions for large span double curvature concrete shells. The present paper also introduces several algorithm improvements dedicated to real-time, clash-free, complex surface decomposition for unfolding and fabrication from thin sheet material.
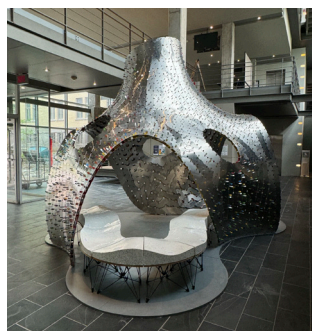
ACKNOWLEDEGMENTS

REFERENCES

Ayres, Phil, Petras Vestartas, and Mette Ramsgaard Thomsen. 2018. 'Enlisting Clustering and Graph-Traversal Methods for Cutting Pattern and Net Topology Design in Pneumatic Hybrids'. In Humanizing Digital Reality: Design Modelling Symposium Paris 2017, 285–94. Springer.

Bechert, Simon, Daniel Sonntag, Lotte Aldinger, and Jan Knippers. 2021. 'Integrative Structural Design and Engineering Methods for Segmented Timber Shells - BUGA Wood Pavilion'. Structures 34:4814–33. https://doi.org/10.1016/j.istruc.2021.10.032.

Eigensatz, Michael, Mario Deuss, Alexander Schiftner, Martin Kilian, Niloy J Mitra, Helmut Pottmann, and Mark Pauly. 2010. 'Case Studies in Cost-Optimized Paneling of Architectural Freeform Surfaces'. In Advances in Architectural Geometry 2010, 49–72. Springer.

Flöry, Simon, and Helmut Pottmann. 2010. 'Ruled Surfaces for Rationalization and Design in Architecture'.
Fornes, Mark. 2016. 'The Art of the Prototypical'. Architectural Design 86 (2): 60–67.

La Magna, Riccardo, Simon Schleicher, and Jan Knippers. 2016. 'Bending-Active Plates'. Advances in Architectural Geometry 2016:170–87.

Lienhard, Julian, and Jan Knippers. 2015. 'Bending-Active Structures'. BAUTECHNIK 92 (6): 394–402. https://doi.org/10.1002/bate.201500007.

Magna, Riccardo La, Markus Gabler, Steffen Reichert, Tobias Schwinn, Frédéric Waimer, Achim Menges, and Jan Knippers. 2013. 'From Nature to Fabrication: Biomimetic Design Principles for the Production of Complex Spatial Structures'. International Journal of Space Structures 28 (1): 27–39.

Martín-Pastor, Andrés, and Rodrigo García-Alvarado. 2019. 'Developable Wooden Surfaces for Lightweight Architecture: Bio-Dune Pavilion'. Digital Wood Design: Innovative Techniques of Representation in Architectural Design, 1481–1500.

Nejur, Andrei. 2023. 'Structurally Aware Fabrication for Large-Scale, Curved Architectural Skins'. In Advances in Architectural Geometry 2023. Advances in Architectural Geometry. Walter de

12

13

The Cnidaria pavilion Nejur, Szentesi, Taghavifard, Balaban, Harrop

Gruyter GmbH & Co KG.

Nejur, Andrei, and Kyle Steinfeld. 2016. 'IVY Bringing a Weighted-Mesh Representation to Bear on Generative Architectural Design Applications'. In ACADIA 2016, 140–51. Ann Arbor MI: CUMINCAD.

Nejur, Andrei, and Kyle Steinfeld. 2017. 'Ivy: Progress in Developing Practical Applications for a Weighted-Mesh Representation for Use in Generative Architectural Design'. In ACADIA 2017, 446–55. Boston, MA: CUMINCAD.

Nicholas, Paul, David Stasiuk, Esben Nørgaard, Christopher Hutchinson, and Mette Ramsgaard Thomsen. 2016. 'An Integrated Modelling and Toolpathing Approach for a Frameless Stressed Skin Structure, Fabricated Using Robotic Incremental Sheet Forming'. Robotic Fabrication in Architecture, Art and Design 2016, 62–77.

Pottmann, Helmut. 2013. 'Architectural Geometry and Fabrication-Aware Design'. Nexus Network Journal 15 (2): 195–208.

Rossi, Gabriella, and Paul Nicholas. 2018. 'Modelling a Complex Fabrication System: New Design Tools for Doubly Curved Metal Surfaces Fabricated Using the English Wheel'. In Proceedings of eCAADe 2018: Computing for a Better Tomorrow, 811–20.

Rueda, Antonio, José M Noguera, and Carmen Martínez-Cruz. 2013. 'A Flooding Algorithm for Extracting Drainage Networks from Unprocessed Digital Elevation Models'. Computers & Geosciences 59:116–23.

Schleicher, Simon, Andrew Rastetter, Riccardo La Magna, Andreas Schönbrunner, Nicola Haberbosch, and Jan Knippers. 2015. 'Form-Finding and Design Potentials of Bending-Active Plate Structures'. In Modelling Behaviour, 53–63. Springer.

Schling, Eike. 2018. 'Design and Construction of Curved Support Structures with Repetitive Parameters'. In Advances in Architectural Geometry 2018.

Schmieder, Markus, and Peter Mehrtens. 2013. 'Cladding Freeform Surfaces with Curved Metal Panels — a Complete Digital Production Chain'. In Advances in Architectural Geometry 2012, edited by Lars Hesselgren, Shrikant Sharma, Johannes Wallner, Niccolo Baldassini, Philippe Bompas, and Jacques Raynaud, 237–42. Vienna: Springer Vienna.

Stanojevic, Djordje, and Kenryo Takahashi. 2019. 'Strip-Based Double-Layered Lightweight Timber Structure'. Proceedings of IASS Annual Symposia 2019 (11): 1–8.

IMAGE CREDITS
All drawings and images by the authors.

Andrei Nejur is currently associate professor at the University of Montreal's School of Architecture, where he specializes in computational design, material cultures and digital fabrication. He is the director of LAIR the Laboratory for Architecture Informatics and Robotics. He was a visiting scholar at UC Berkeley College of Environmental Design, and a postdoc at University of Pennsylvania Weizman School of Design. Andrei is the author of Ivy for Grasshopper and a co-author of Polyframe for Rhino and Grasshopper

Szende Szentesi-Nejur is an architect and assistant professor at Université Laval's School of Architecture. Her expertise spans building science, environmental performance, and adaptive reuse, with a focus on sustainable design and daylighting strategies. She has extensive professional experience in architectural practice, contributing to notable projects, including educational institutions in Quebec. Szende is actively involved in research exploring the integration of digital design and environmental optimization, aiming to advance sustainable architectural solutions.

Reza Taghavifard is a PhD student with a solid foundation in architectural engineering, holding a bachelor's degree in the field. He furthered his expertise by earning a master's degree in computational design, where his thesis focused on developing AI models for design space exploration. Currently, he is pursuing his PhD at the University of Montreal's Laboratory of Architecture, Informatics, and Robotics (LAIR) where he is developing frameworks to facilitate the fabrication of multi-layer shell structures from sheet materials, optimizing both their structural performance and fabricability.

Thomas Balaban is a Montreal-based architect, educator, and researcher. He is a partner at TBA and an associate professor at l'École d'architecture, Université de Montréal. His inventive practice explores the intersection of contemporary architecture and the urban environment. His teaching and research focus on representation, design using digital tools, and how machines can help build the future. In 2021, Balaban co-curated Impostor Cities, Canada's presentation at the 17th Venice Architecture Biennale, later exhibited at the Museum of Contemporary Art Toronto. He knows his craft, and he works at it.

Patrick Harrop is an invited professor at University of Montreal's School of Architecture. Patrick Harrop's artistic practice is a research / creation based synthetic exploration of the material impact of technology both in the historical canon of architectural work as well as the engagement with contemporary technology. His research specialty is in emerging technology and design with a particular emphasis in electromechanical hacking, digital fabrication and open-source maker culture. He is currently a member artist and former president of Perte de Signal, artist run center in Montreal as well as a licensed architect with the OAQ.

TOPIC (ACADIA team will fill in)